University of Glasgow

Todorova, B. N. and Steijl, R. (2019) Derivation and numerical comparison of Shakhov and Ellipsoidal Statistical kinetic models for a monoatomic gas mixture. *European Journal of Mechanics - B/Fluids*, 76, pp. 390-402. (doi:10.1016/j.euromechflu.2019.04.001)

There may be differences between this version and the published version. You are advised to consult the publisher's version if you wish to cite from it.

http://eprints.gla.ac.uk/183360/

Deposited on: 02 April 2019

Enlighten – Research publications by members of the University of Glasgow
http://eprints.gla.ac.uk

Journal

Derivation and Numerical Comparison of Shakhov and Ellipsoidal Statistical Kinetic Models for a Monoatomic Gas Mixture

Blaga N. Todorova[1] and René Steijl*[2]

[1]*School of Engineering, University of Glasgow, Scotland, United Kingdom*
[2]*School of Engineering, University of Glasgow, Scotland, United Kingdom*

Summary

Gas mixtures are important for many practical applications. Extending kinetic model equations of the Bhatnagar-Gross-Krook (BGK) type from a single-species gas to a multi-species gas mixture presents a number of significant challenges. First, obtaining the correct species diffusions, viscous stresses as well as heat conduction in the continuum limit requires a careful design of the collision terms in the kinetic equations. Secondly, the derived model collision terms need to guarantee positivity of the macroscopic fields.

In the present work, two new kinetic models are introduced and compared: an approach based on the Shakhov kinetic model and an approach involving an anisotropic Gaussian equilibrium function. The two new models are capable of modelling a binary mixture of monoatomic gases, with updated definitions for the relaxation parameters and target species velocities and temperature. Both methods account for separate species-mean velocity such that the species diffusion and velocity drift are accurately represented. The key contribution of the models is the exact recovery of the Fick, Newton and Fourier laws in the continuum limit, while preserving positive temperature fields and crucial properties of the Boltzmann equation.

The profile of a normal shock wave is inspected under various flow conditions to numerically validate the two models. The results show improvement upon comparison with a model, which has two correct transport coefficients, and demonstrate the ability to reliably model inert gas mixtures.

Keywords: Kinetic models, gas mixture, transport properties, species diffusion, normal shock wave

1 Introduction

The Boltzmann equation [13] is a fundamental equation of gas dynamics. It can accurately characterize any flow regime- from continuum through transitional to free molecular flow and can easily be extended to inert gas mixtures [13]. The direct simulation Monte Carlo (DSMC) method [6] [34] [27] is widely studied and statistically approximates solutions to the Boltzmann equation. The limitations of the method occur when the flow is approaching continuum regime and lower speeds. Alternatively, the discrete velocity method (DVM) [32] is a deterministic approach, which leads to accuracy in all flow regimes and no statistical noise, but the memory overhead and the required computational time limits the range of possible applications. The described problems are caused by the collision term on the right hand side, which presents a numerical challenge in terms of modelling and computational cost.

Consequently, the complex collision integral of the Boltzmann equation is substituted by the BGK relaxation model [5], which preserves the most important mathematical and physical characteristics of the full equation close to equilibrium. This model has a simplified mathematical form and is widely applied in numerical simulations, e.g. [41][42]. However, the BGK model cannot concurrently determine the correct viscous and heat transfer coefficients in the hydrodynamic limit and thus the Prandtl number is not correct. For monoatomic gas, the issue has been addressed in two ways- the Shakhov BGK model [33] and the Ellipsoidal Statistical (ES) BGK model [26]. Both models modify the Maxwellian distribution function in the original BGK model to receive a new target equilibrium function to rectify Prandtl number. Both corrections behave well in the asymptotic continuum limit and the Navier-Stokes equations can be derived through the Chapman-Enskog expansion. The Shakhov model has shown to be more reliable for strong non-equilibrium conditions [14], while the ES-BGK has been investigated more thoroughly mathematically to confirm non-negativity of the distribution function and the macroscopic fields [3][10][11].

The extension of the kinetic model equations to gas mixtures is not trivial and resorting to relaxation models presents a substantial difficulty. Some of the challenges are outlined- e.g. there is momentum and energy exchange between species and therefore the conservation equations are for the whole system. The hydrodynamic limit involves species diffusion and the number of transport coefficients for monoatomic binary mixtures increases to five - Fick, Soret, Dufour, Fourier and viscosity coefficients. Besides, the simplified collision term can lead to non-physical effects as a negative distribution function and negative density or temperature regions. Mixture BGK-type approximation for a Maxwellian potential[20][36][31][22] and later on for an arbitrary potential [17] have been developed and confirm the obstacles mentioned. A common weakness of these models is the breakdown of the indifferentiability principle, which has been defined and overcome for an arbitrary potential [16], however reintroducing the negativity problem. Finally,

[0]*Corresponding author: René Steijl, James Watt South Building, Glasgow G12 8QQ. Email: rene.steijl@glasgow.ac.uk

Andries et al. [1] formulated a consistent BGK mixture model, preserving positive continuum fields and distributions, complying with the indifferentiability principle and considering entropy decay. There are two types of Boltzmann derived models for mixtures in regard to the formulation of the collision term of the transport equation. The AAP model [1] is a single-relaxation based model, treating self- and cross-collisions with one operator on the right-hand side of the equation. Another possible approach is to have a sum of collision operators, similar to the full Boltzmann equation and model each collision type individually [29] [21]. A detailed comparison of the mathematical properties of the two types of models is presented by Klingenberg et al. [28] and Bobylev et al. [7]. The single relaxation operator with a single relaxation time is widely applied, since it provides simplicity and reduced computational cost of the numerical schemes. A similar formulation to the AAP model is defined by Groppi et al. [19]. Both models introduce modified species velocity and temperature in the equilibrium distribution function that differ from the species mean velocity and temperature. These modified quantities recover the correct total momentum and energy of the system and are directly related to the species mean variables. An advantage of the model by Groppi et al. is that it contains two relaxation coefficients, capable of fitting two of the transport coefficients correctly, leading to true diffusion and viscosity. The model also guarantees positive macroscopic fields. The kinetic models introduced in this paper are based on the Groppi et al. model, described in greater detail in the next section. Similarly, Brull's BGK mixture model [9] also has species mean velocity defining the velocity distribution function. The model targets the fit of the diffusion and viscosity coefficients, but requires further work to have a correct Prandtl number. The latest ES-BGK mixture model by Brull [8] has a common mixture velocity in the species distribution function. Two relaxation coefficients recover the exact viscosity and heat flux of the system. However, as outlined in the paper, the value of the Fick coefficient is calculated according to the new model, but remains incorrect. A new consistent BGK mixture model was introduced recently [7]. Both Maxwellian and arbitrary potential molecules are considered in the presented model. For an arbitrary number of species, this model was shown to fulfill all consistency requirements concerning conservation laws, equilibria and H-theorem. The number of correctly fitted transport coefficients is not detailed in this work.

Based on the work by Groppi et al. [19], we have modified the equilibrium distribution function by incorporating a Shakhov-type correction. A second model involves an ES-type extension. The two new models are capable of modelling a binary mixture of monoatomic gases, with updated definitions for the relaxation parameters and target species velocities and temperature. Both methods account for separate species-mean velocity such that the species diffusion and velocity drift are accurately represented. The Chapman-Enskog procedure is followed to derive the asymptotic hydrodynamic limit and provide expressions for viscosity, thermal conductivity and diffusion coefficients. The two model extensions provide an extra relaxation parameter that allows for the correct fit of the three coefficients. The novelty of the two newly-introduced models lies in the capability to capture one extra transport property in the

continuum limit in comparison to the existing kinetic mixture models, e.g. [8, 9, 19]. The Shakhov single-species and ES single-species models that address the Prandtl number problem in the single-species BGK models are well understood. However, so far these approaches have not been applied to gas mixtures. In this paper the Shakhov- and ES-based extensions correct the Prandtl number for a binary mixture kinetic model. This is a significant improvement and is the key to the demonstrated good numerical results. The models enjoy good mathematical properties, including conservation of mass, momentum and energy, indifferentiability condition and more specifically for the ES-based model the H-theorem and the equilibrium state are shown. In summary, the main contribution is the introduction of two kinetic models, with three correct transport coefficients, that are theoretically and numerically evaluated.

The numerical validation of the kinetic models is based on the simplest test case of non-equilibrium flow- the normal shock wave. Under this flow condition, there are strong gradients of the macroscopic variables and the species show disjoint behaviour. The profile of a shock wave for a monoatomic gas mixture is a well-studied problem both experimentally [12] [23] and numerically [30] [40] [37] [43], etc. The work by Kosuge et al. [30] , which is based on the Boltzmann transport equation, is considered a standard benchmark and all numerical studies compare with it. The introduced kinetic models are solved using the DVM approach and the results are validated with Kosuge et al.

The structure of the paper is as follows. In section 2 we summarize classical properties of single-relaxation models for gas mixtures. Key elements of the work by Groppi et al. [19] are discussed in section 3. Sections 4 and 5 introduce the two kinetic models, while their properties and hydrodynamic limit are shown in sections 6 and 7 respectively. The transport coefficients in the continuum limit are discussed in detail in section 8. The methodology (Sec. 9) and the results (Sec. 10) of the numerical analysis are presented, followed by concluding remarks (Sec. 11).

2 BGK mixture model

The following properties are standard for kinetic mixture models. They are inherent of the Boltzmann equation and provide consistency between the full equation and the simplified relaxation models. The evolution of the species-specific distribution function is governed by the BGK relaxation equation:

$$\frac{\partial f_s}{\partial t} + \underline{u} \cdot \nabla_{\underline{x}} f_s = Q_s\big[f_1, f_2\big] \quad ; \quad s = 1, 2 \tag{1}$$

with collision terms $Q_s\big[f_1, f_2\big]$ and $\underline{u}$ the particle velocity. The simplification of the kinetic equations lies in the substitution of the complex collision integral of the Boltzmann equation with the relaxation term $Q_s\big[f_1, f_2\big]$, expressed by the relaxation rate of the difference between the equilibrium and non-equilibrium state. The target equilibrium function varies between kinetic models and determines some of the main properties. However, a necessary condition for all models is that the collision term preserves mass, momentum and energy. Note that since the gas is a chemically

inert mixture, mass conservation is per species, while momentum and energy can be exchanged between them and it is only the sum that needs to be conserved. Therefore, the following constraints on the collision operator are imposed:

$$\begin{aligned}
&\iiint_{-\infty}^{\infty} Q_s d\underline{u} = 0 \quad ; \quad s = 1,2 \\
&\sum_{s=1}^{2} \iiint_{-\infty}^{\infty} m_s \underline{u} Q_s d\underline{u} = 0 \\
&\sum_{s=1}^{2} \iiint_{-\infty}^{\infty} \frac{1}{2} m_s |\underline{u}|^2 Q_s d\underline{u} = 0
\end{aligned} \tag{2}$$

where $d\underline{u} = dudvdw$. We denote with n_s, ρ_s, u_s and T_s the species macroscopic quantities- number density, density, mean velocity and temperature of a species s. They are found as moments of the nonequilibrium distribution function f_s:

$$\begin{aligned}
n_s &= \iiint_{-\infty}^{\infty} f_s d\underline{u} \\
n_s \underline{u}_s &= \iiint_{-\infty}^{\infty} \underline{u} f_s d\underline{u} \\
\frac{3}{2} n_s k T_s &= \frac{m_s}{2} \iiint_{-\infty}^{\infty} (\underline{u} - \underline{u}_s)^2 f_s d\underline{u}
\end{aligned} \tag{3}$$

where k is the Boltzmann constant. From the species macroscopic variables, the overall gas mixture properties n, ρ, $\underline{u}_0$ and T are obtained:

$$n = \sum_{s=1}^{2} n_s \quad ; \quad \rho = \sum_{s=1}^{2} \rho_s \quad ; \quad \underline{u}_0 = \frac{1}{\rho} \sum_{s=1}^{2} \rho_s \underline{u}_s \quad ; \quad \sum_{s=1}^{2} \rho_s \big(\underline{u}_s - \underline{u}_0\big)^2 = \sum_{s=1}^{2} \rho_s |\underline{u}_s|^2 - \rho |\underline{u}_0|^2 \tag{4}$$

$$\frac{3}{2} n k T = \sum_{s=1}^{2} \frac{3}{2} n_s k T_s + \frac{1}{2} \sum_{s=1}^{2} \rho_s \big(\underline{u}_s - \underline{u}_0\big)^2 \tag{5}$$

The equilibrium solution is defined by the Maxwellian distributions as functions of common macroscopic velocity ($\underline{u}_0$) and gas temperature (T), and number densities n_s for each species.

$$f_s^M(\underline{u}) = n_s \left(\frac{m_s}{2\pi k T} \right)^{3/2} \exp\left[- \frac{m_s}{2kT} \big(\underline{u} - \underline{u}_0\big)^2 \right] \tag{6}$$

3 Groppi et al's model

The two new kinetic models introduced in this paper build upon the work by Groppi et al. [19]. This section summarizes their work and allows for a comparison of the key equations between the models, including definitions of the distribution function, target species velocity and temperature.

The collision term involves a common relaxation rate ν as a standard single relaxation model, but the equilibrium distribution function f_s^M is substituted with the modified distribution function G_s, leading to the following expression for Q_s:

$$Q_s = \nu\big(G_s - f_s\big) \quad ; \quad s = 1, 2 \tag{7}$$

The modified function allows for species drift velocities $\underline{u}_s^{(g)}$ and common modified temperature $\hat{T}$ that are different from the local gas mixture velocity and temperature and is in the form:

$$G_s(\underline{u}) \,=\, n_s\bigg(\frac{m_s}{2\pi k\hat{T}}\bigg)^{3/2}\exp\bigg[-\frac{m_s}{2k\hat{T}}\Big(\underline{u}-\underline{u}_s^{(g)}\Big)^2\bigg] \tag{8}$$

The main advantage of Groppi et al's model is the introduction of a second relaxation parameter η, which sets a constraint on the species drift velocity equalization.

$$\frac{1}{n_1}\iiint_{-\infty}^{\infty}\underline{u}Q_1 d\underline{u} - \frac{1}{n_2}\iiint_{-\infty}^{\infty}\underline{u}Q_2 d\underline{u} = -\eta\big(\underline{u}_1 - \underline{u}_2\big) \tag{9}$$

Evaluating the above integrals and following the moment conservation equation, the species target velocity in G_s is expressed from the local species velocity and the average gas mixture velocity.

$$\underline{u}_s^{(g)} = \Big(1-\frac{\eta}{\nu}\Big)\underline{u}_s + \frac{\eta}{\nu}\underline{u}_0 \quad ; \quad s = 1, 2 \tag{10}$$

The same principle is applied with the energy conservation equation to express the modified temperature in the equilibrium functions G_s:

$$\hat{T} \,=\, T - \frac{1}{3nk}\sum_{s=1}^{2}\rho_s\big(\underline{u}_s^{(g)} - \underline{u}_0\big)^2 = T - \frac{1}{3nk}\Big(1-\frac{\eta}{\nu}\Big)^2\sum_{s=1}^{2}\rho_s\big(\underline{u}_s - \underline{u}_0\big)^2 \tag{11}$$

As demonstrated in the original paper [19] the relaxation ratio is limited in the bounds $0 \leq \eta/\nu \leq 2$ to ensure positive temperature fields. The second relaxation coefficient allows for two transport coefficients to be recovered correctly in

the hydrodynamic limit: the Fick and viscosity coefficients. Building upon the discussed model, we aim to fit three transport coefficients with two different approaches, discussed in the next sections.

4 Shakhov-based model

A Shakhov-type correction is applied to extend the kinetic model in order to correct the Prandtl number. The Prandtl number of a binary mixture has previously been examined [18],[4],[35]. The values it takes depend on the mass ratio between species and the concentration levels. For high mass ratios (e.g helium-krypton mix with mass ratio of 21) and equal species concentration, the Prandtl number can drop to values as low as $Pr_{mix} = 1/5$, while the maximum values for a monoatomic gas are reached when the gas is pure, leading to $Pr_{mix} = Pr = 2/3$. In theory increasing the mass ratio further will lead the Prandtl number close to 0 and therefore the limits of the Pr_{mix} for monoatomic gases are $Pr_{mix} \in (0, 2/3]$. The expression for the mixture Prandtl number is discussed further in Section 8.
The Shakhov model [33] modifies the Maxwellian distribution function by introducing a heat flux correction. Similarly, expanding the described Gaussian distribution (Eq. 8), a new equilibrium distribution function is introduced:

$$G_s^{Sh}(\underline{u}) = \underbrace{n_s\left(\frac{m_s}{2\pi k\hat{T}}\right)^{3/2}\exp\left[-\frac{m_s}{2k\hat{T}}\left(\underline{u}-\underline{u}_s^{(g)}\right)^2\right]}_{G_s(\underline{u})}\left\{1+\frac{2\big(1-Pr\big)\big(\underline{u}-\underline{u}_s^{(g)}\big)\cdot\underline{q}_s^{corr}}{5p_sk\hat{T}/m_s}\left[\frac{m_s}{2k\hat{T}}\left(\underline{u}-\underline{u}_s^{(g)}\right)^2-\frac{5}{2}\right]\right\} \quad (12)$$

with species pressure p_s defined as $p_s = \rho_s k\hat{T}/m_s = n_s k\hat{T}$ and Pr is a target Prandtl number.

In the single species Shakhov model, the heat flux correction $\underline{q}^{corr}$, which goes into the distribution function, is the full heat flux. This represents the Fourier conduction law. It is computed by taking the moment of the non-equilibrium distribution function with respect to the mean gas velocity $\frac{1}{2}m(\underline{u}-\underline{u}_0)(\underline{u}-\underline{u}_0)^2$. For a mixture of gases, the heat flux of the gas comprises of energy flux based on the temperature gradient (thermal conductivity) and the mass gradient (the Dufour effect). However, the introduced Shakhov correction is not affected by the coupled effect, but only from the direct effect of energy flux, dependent on the temperature gradient. To achieve a heat flux correction $\underline{q}_s^{corr}$ that involves only the Fourier effect, the moments of the non-equilibrium distribution function f_s^ϵ are taken with respect to the species mean velocity: $\frac{1}{2}m_s(\underline{u}-\underline{u}_s)(\underline{u}-\underline{u}_s)^2$. The expression for f_s^ϵ comes from the Chapman-Enskog expansion up to $O(\epsilon^2)$ order (see Eq. (40) and Eq. (41)).

$$\iiint_{-\infty}^{\infty} m_s(\underline{u}-\underline{u}_s)\frac{1}{2}(\underline{u}-\underline{u}_s)^2 f_s^\epsilon d\underline{u} = \iiint_{-\infty}^{\infty} m_s(\underline{u}-\underline{u}_s)\frac{1}{2}(\underline{u}-\underline{u}_s)^2\Big\{G_s^{Sh}-\frac{\epsilon}{\nu}\Big(\frac{\partial f_s^M}{\partial t}+\underline{u}\frac{\partial f_s^M}{\partial \underline{x}}\Big)\Big\}d\underline{u}+O(\epsilon^2)$$

In the continuum limit the integration yields:

$$\iiint_{-\infty}^{\infty} m_s(\underline{u}-\underline{u}_s)\frac{1}{2}(\underline{u}-\underline{u}_s)^2 G_s^{Sh} d\underline{u} = \frac{5}{2}n_s kT\big(\underline{u}_s^{(g)}-\underline{u}_s\big) + (1-Pr)\underline{q}_s^{corr} + O(\epsilon^2)$$

$$\iiint_{-\infty}^{\infty} m_s(\underline{u}-\underline{u}_s)\frac{1}{2}\big(\underline{u}-\underline{u}_s\big)^2\Big\{-\frac{\epsilon}{\nu}\Big(\frac{\partial f_s^M}{\partial t}+\underline{u}\frac{\partial f_s^M}{\partial \underline{x}}\Big)\Big\}d\underline{u} = \frac{\eta}{\nu}\frac{5}{2}n_s kT(\underline{u}_s-\underline{u}_0) - \frac{\epsilon}{\nu}\frac{5}{2}k\frac{n_s kT}{m_s}\frac{\partial T}{\partial \underline{x}} + O(\epsilon^2) \quad (13)$$

where ϵ represents a small parameter, corresponding to the Knudsen number, used in the Chapman-Enskog expansion (see Appendix C). Combining the two parts of the integration and substituting the expression for $u_s^{(g)}$ (Eq. 15) leads to the expression for the heat flux correction.

$$\underline{q}_s^{corr} = -\frac{\epsilon}{\nu}\frac{5}{2}k\frac{n_s kT}{m_s}\frac{\partial T}{\partial \underline{x}} + (1-Pr)\underline{q}_s^{corr} + O(\epsilon^2) \quad (14)$$

$$\underline{q}_s^{corr} = -\frac{\epsilon}{\nu}\frac{5}{2}\frac{k}{Pr}\frac{n_s kT}{m_s}\frac{\partial T}{\partial \underline{x}} + O(\epsilon^2)$$

The moments of the extended distribution function G_s^{Sh} are unchanged up to and including second order in molecular velocity in comparison to Groppi et al.'s model. As expected from a Shakhov-type correction, only the third order moments are affected with a correction on the heat flux with the Prandtl number (see Appendix A). Therefore, the expressions for $\underline{u}_s^{(g)}$ and $\hat{T}$ are unchanged in comparison to the original model (Eq. 10 and Eq. 11).

$$\underline{u}_s^{(g)} = \Big(1-\frac{\eta}{\nu}\Big)\underline{u}_s + \frac{\eta}{\nu}\underline{u}_0 \quad ; \quad s=1,2 \quad (15)$$

From the energy conservation, the modified temperature in the distribution function G_s^{Sh} is expressed:

$$\hat{T} = T - \frac{1}{3nk}\sum_{s=1}^{2}\rho_s\big(\underline{u}_s^{(g)}-\underline{u}_0\big)^2 = T - \frac{1}{3nk}\Big(1-\frac{\eta}{\nu}\Big)^2\sum_{s=1}^{2}\rho_s\big(\underline{u}_s-\underline{u}_0\big)^2 \quad (16)$$

$$nk\hat{T} = \sum_{s=1}^{2}n_s kT_s + \frac{1}{3}\left[\frac{\eta}{\nu}\Big(2-\frac{\eta}{\nu}\Big)\sum_{s=1}^{2}\rho_s\big(\underline{u}_s-\underline{u}_0\big)^2\right] \quad (17)$$

As in the original model the relaxation ratio is restricted between $0 \le \eta/\nu \le 2$ in order to preserve the positivity of temperature fields.

5 ES-based model

Starting from the same original distribution function (Eq. 8), an anisotropic modification is formulated, following the approach used for the single species ES model [26] . The new distribution function is defined as:

$$G_s^{ES}(\underline{u}) = \frac{n_s}{\sqrt{det(2\pi\underline{\underline{\Lambda}}_s)}}\exp\Big[-\frac{1}{2}\big(\underline{u}-\underline{u}_s^{(g)}\big)\cdot\underline{\underline{\Lambda}}_s^{-1}\cdot\big(\underline{u}-\underline{u}_s^{(g)}\big)\Big] \tag{18}$$

The separate drift velocity $\underline{u}_s^{(g)}$ for each species is kept as in the isotropic Gaussian, while the tensor $\underline{\underline{\Lambda}}_s$ is introduced by the temperature $\hat{T}$ and the ES relaxation parameter ν_{ES} (see Appendix B):

$$\underline{\underline{\Lambda}}_s = \nu_{ES}\underline{\underline{\Theta}}_s + \big(1-\nu_{ES}\big)\Big(\frac{k\hat{T}}{m_s}\Big)\underline{\underline{I}} \tag{19}$$

where the tensor $\underline{\underline{\Theta}}_s$ is also based on the species drift velocity $\underline{u}_s^{(g)}$ as:

$$\underline{\underline{\Theta}}_s = \frac{1}{n_s}\iiint_{-\infty}^{\infty}\big(\underline{u}-\underline{u}_s^{(g)}\big)\otimes\big(\underline{u}-\underline{u}_s^{(g)}\big)f_s d\underline{u} \tag{20}$$

The collision operator is also altered with the relaxation parameter ν_{ES} and is in the form:

$$Q_s = \frac{\nu}{1-\nu_{ES}}\big(G_s - f_s\big) \quad ; \quad s = 1,2 \tag{21}$$

where the expression for ν_{ES} is bound by the Prandtl number and $Pr = \frac{1}{1-\nu_{ES}}$ as in [3]. For monoatomic gases the parameter $Pr = 2/3$, which leads to $\nu_{ES} = -1/2$. This value assures the mixture Prandtl number Pr_{mix} has a correct behavior in the limit of a pure monoatomic gas for the ES-based model, as demonstrated in Section 8. Therefore, following the relaxation between velocities, introduced by Groppi and co-workers (Eq. (9)):

$$\frac{1}{n_1}\iiint_{-\infty}^{\infty}\underline{u}Q_1 d\underline{u} - \frac{1}{n_2}\iiint_{-\infty}^{\infty}\underline{u}Q_2 d\underline{u} = -\eta\big(\underline{u}_1-\underline{u}_2\big) \tag{22}$$

leads to a modified relaxation of the mean species velocities:

$$\begin{aligned}\frac{\nu}{1-\nu_{ES}}\Big[\big(\underline{u}_1^{(g)}-\underline{u}_1\big)-\big(\underline{u}_2^{(g)}-\underline{u}_2\big)\Big] &= -\eta\big(\underline{u}_1-\underline{u}_2\big) \\ \Rightarrow \underline{u}_1^{(g)}-\underline{u}_2^{(g)} &= \Big(1-\frac{\eta}{\nu}(1-\nu_{ES})\Big)\big(\underline{u}_1-\underline{u}_2\big)\end{aligned} \tag{23}$$

To finalize the definition of the new kinetic model, we examine the expressions for the species modified velocity and temperature. The formulation of $\underline{u}_s^{(g)}$ is now changed to accommodate for the relaxation parameter, characteristic for the ES model ν_{ES}.

$$\underline{u}_s^{(g)} = \Big(1 - \frac{\eta}{\nu}(1-\nu_{ES})\Big)\underline{u}_s + \frac{\eta}{\nu}(1-\nu_{ES})\underline{u}_0 \quad ; \quad s = 1,2 \tag{24}$$

The common target temperature $\hat{T}$ is also required to change to provide an energy conserving model.

$$\hat{T} = T - \frac{1}{3nk(1-\nu_{ES})}\left[\sum_{s=1}^{2}\rho_s\big(\underline{u}_s^{(g)} - \underline{u}_0\big)^2 - \nu_{ES}\sum_{s=1}^{2}\rho_s\big(\underline{u}_s - \underline{u}_0\big)^2 + \nu_{ES}\sum_{s=1}^{2}\rho_s\big(\underline{u}_s^{(g)} - \underline{u}_s\big)^2\right] \tag{25}$$

The expression for $\hat{T}$ as a function of the mean species and gas velocities is obtained by substituting $\underline{u}_s^{(g)}$ from equation (24) into (25).

$$\hat{T} = T - \frac{1}{3nk}\left[\Big(1 - \frac{\eta}{\nu}(1-\nu_{ES})\Big)^2\sum_{s=1}^{2}\rho_s\big(\underline{u}_s - \underline{u}_0\big)^2\right] \tag{26}$$

A comparison with the original expression for $\hat{T}$ (Eq. (11)) shows that the additional term comes from the relaxation change ν_{ES} introduced by the ES correction. Setting $\nu_{ES} = 0$ will eliminate the difference and the equations will reduce to Groppi et al.'s model. This is also true for the Shakhov-based model when $Pr = 1$. Notice that:

$$nk\hat{T} = \sum_{s=1}^{2} n_s k T_s + \frac{1}{3}\left[\frac{\eta}{\nu}(1-\nu_{ES})\Big(2 - \frac{\eta}{\nu}(1-\nu_{ES})\Big)\sum_{s=1}^{2}\rho_s\big(\underline{u}_s - \underline{u}_0\big)^2\right] \tag{27}$$

To guarantee positive temperature the fraction η/ν is in the limits $0 \leq \eta/\nu \leq 2/(1-\nu_{ES})$. In comparison to the Groppi model the possible range for the relaxation parameter η is more restrictive due to the introduction of ν_{ES} with maximum value of $\eta/\nu = 4/3$ when the maximum for $\nu_{ES} = -0.5$ for a monoatomic binary mixture is reached. The fundamental properties derived for the Boltzmann model need to be satisfied by the kinetic models. For a gas mixture, these include the H-theorem, the equilibrium state, indifferentiability principle, collision invariants and continuum limit and are discussed in the following sections.

6 Properties

6.1 H-functional

The entropy of a system increases constantly until it reaches its maximum at the equilibrium level. The H theorem is an a priori statement that guarantees the second law of thermodynamics is preserved and is shown for the ES-based model. For a binary gas mixture:

$$H = \sum_{s=1}^{2} \iiint_{-\infty}^{\infty} (f_s ln f_s - f_s) d\underline{u} \tag{28}$$

We will prove that:

$$\frac{\partial H}{\partial t} = \frac{\partial}{\partial t} \sum_{s=1}^{2} \iiint_{-\infty}^{\infty} (f_s ln f_s - f_s) d\underline{u} \leq 0 \tag{29}$$

The LHS of Eq. (29) can be simplified as:

$$\frac{\partial}{\partial t} \sum_{s=1}^{2} \iiint_{-\infty}^{\infty} (f_s ln f_s - f_s) d\underline{u} = \sum_{s=1}^{2} \iiint_{-\infty}^{\infty} \frac{\partial}{\partial t} (f_s ln f_s - f_s) d\underline{u} = \sum_{s=1}^{2} \iiint_{-\infty}^{\infty} \frac{\partial f_s}{\partial t} ln f_s d\underline{u} \tag{30}$$

The governing equation for the ES-based model for a spatially uniform problem allows to express the derivative of f_s:

$$\frac{\partial f_s}{\partial t} = \frac{\nu}{1 - \nu_{ES}} (G_s^{ES} - f_s) \quad ; \quad s = 1, 2 \tag{31}$$

$$\frac{\partial}{\partial t} \sum_{s=1}^{2} \iiint_{-\infty}^{\infty} (f_s ln f_s - f_s) d\underline{u} = \sum_{s=1}^{2} \iiint_{-\infty}^{\infty} \frac{\nu}{1 - \nu_{ES}} (G_s^{ES} - f_s) ln f_s d\underline{u} \tag{32}$$

Since $H(x) = xlnx - x$ is a strictly convex function for $x > 0$ and $H'(x) = lnx$ it follows that for $x = f_s$:

$$\sum_{s=1}^{2} \iiint_{-\infty}^{\infty} (G_s^{ES} - f_s) ln f_s d\underline{u} \leq H(G_s^{ES}) - H(f_s) \tag{33}$$

It is sufficient to prove that $H(G_s^{ES}) \leq H(f_s)$. This is a challenging derivation and it is better to consider the following process $H(G_s^{ES}) \leq H(G_s^{\overline{\Theta}_s}) \leq H(G_s) \leq H(f_s)$.

The first two inequalities are deduced by analogy with the formal derivation of the ES BGK model [3], where the

velocity is $u_s^{(g)}$, the temperature- $\hat{T}$, $\underline{\underline{\Lambda}}_s$ and $\underline{\underline{\Theta}}_s$ are functions of $u_s^{(g)}$ and $\hat{T}$. The distribution functions G_s^{ES} and G_s are defined as before (see Eq. (18) and Eq. (8) respectively) and $G_s^{\underline{\underline{\Theta}}_s}$ expressed from the tensor $\underline{\underline{\Theta}}_s$ for $\nu_{ES} = 1$ as:

$$G_s^{\underline{\underline{\Theta}}_s} = \frac{n_s}{\sqrt{det(2\pi\underline{\underline{\Theta}}_s)}} \exp\Big[-\frac{1}{2}\big(\underline{u} - \underline{u}_s^{(g)}\big)\cdot\underline{\underline{\Theta}}_s^{-1}\cdot\big(\underline{u} - \underline{u}_s^{(g)}\big)\Big] \tag{34}$$

Following [3]:

$$H(G_s^{ES}) - H(G_s^{\underline{\underline{\Theta}}_s}) = \frac{1}{2}\sum_{s=1}^{2} n_s ln \frac{det\ \underline{\underline{\Theta}}_s}{det\ \underline{\underline{\Lambda}}_s} \tag{35}$$

If the RHS of the equation is negative, $H(G_s^{ES}) \leq H(G_s^{\underline{\underline{\Theta}}_s})$ follows. This is achieved only if $det\ \underline{\underline{\Lambda}}_s \geq det\ \underline{\underline{\Theta}}_s$, the detailed derivation of which can be found in [2],[3]. In [2] and the reference therein state the classical result that the entropy at a given velocity, number density and pressure tensor ($\underline{\underline{\Theta}}_s$) is minimized for the Gaussian defined by that pressure tensor and therefore $H(G_s^{\underline{\underline{\Theta}}_s}) \leq H(G_s)$.

The final inequality ($H(G_s) \leq H(f_s)$) follows the proof of the H function by the original model [19], but with the new definition of $u_s^{(g)}$ and the allowed range of the relaxation parameter $0 < \eta < 2\nu/(1-\nu_{ES})$. This is done by the direct evaluation of $H(G_s)$ and $H(f_s)$, where the entropy evaluated at the local Maxwellian (f_s^{LocM}) with the same variables of the non-equilibrium f_s (u_s, n_s and T_s) is $H(f_s^{LocM})$ and is less than the entropy $H(f_s)$.

$$\begin{aligned} H(G_s) &= \sum_{s=1}^{2} n_s\left(ln(n_s) + \frac{3}{2}ln\left(\frac{m_s}{2\pi k\hat{T}}\right)\right) - n \\ H(f_s) \geq H(f_s^{LocM}) &= \sum_{s=1}^{2} n_s\left(ln(n_s) + \frac{3}{2}ln\left(\frac{m_s}{2\pi kT_s}\right)\right) - n \\ &\Rightarrow H(G_s) - H(f_s) \leq \sum_{s=1}^{2}\frac{3}{2}n_s ln\left(\frac{T_s}{\hat{T}}\right) \leq \frac{3}{2\hat{T}}\left(\sum_{s=1}^{2} n_s T_s - n\hat{T}\right) \end{aligned} \tag{36}$$

The last inequality is due to the second order Taylor expansion for lnT_s, centered at $\hat{T}$: ($lnT_s \leq ln\hat{T} + (T_s - \hat{T})/\hat{T}$). From Eq. (26) and for the allowed range of η, it follows that $n\hat{T} \geq \sum_{s=1}^{2} n_s T_s$ and therefore $H(G_s) \leq H(f_s)$.

Since $H(G_s^{ES}) \leq H(G_s^{\underline{\underline{\Theta}}_s}) \leq H(G_s) \leq H(f_s)$ then $H(G_s^{ES}) - H(f_s) \leq 0$.

$$\begin{aligned} \frac{\partial}{\partial t}\sum_{s=1}^{2}\iiint_{-\infty}^{\infty}(f_s ln f_s - f_s)d\underline{u} &\leq \frac{\nu}{1-\nu_{ES}}(H(G_s^{ES}) - H(f_s)) \leq 0 \\ &\Longrightarrow \frac{\partial H}{\partial t} \leq 0 \end{aligned} \tag{37}$$

6.2 Equilibrium

The entropy of a gas increases with time and reaches maximum at equilibrium. To achieve the equality of the H-functional, a necessary condition is $(H(G_s^{ES}) - H(f_s^{LocM})) = 0$, which can be expanded as:

$$\underbrace{H(G_s^{ES}) - H(G_s)} + \underbrace{H(G_s) - H(f_s^{LocM})} = 0 \tag{38}$$

Since both expressions are non-positive, in order to satisfy the equation, each one needs to be 0. It follows that $H(G_s^{ES}) - H(G_s) = 0$ and $H(G_s) - H(f_s^M) = 0$ or $H(G_s^{ES}) = H(G_s)$ and $H(G_s) = H(f_s^M)$. The first equality is based on $H(G_s^{ES}) = H(G_s^{\Theta_s}) = H(G_s)$, following the single species Ellipsoidal model [3]. The entropies $H(G_s^{ES}) = H(G_s^{\Theta_s})$ are equal only if $det\ \underline{\underline{\Lambda}}_s = det\ \underline{\underline{\Theta}}_s$ according to Eq. (35), from which the eigenvalues expression follows: $\lambda_1^s = \lambda_2^s = \lambda_3^s = \frac{k}{m_s}\hat{T}$. The entropies $H(G_{\underline{\underline{s}}}^{\underline{\underline{\Theta}}_s}) = H(G_s)$ are equal when G_s is expressed from the Gaussian structure and equal to $G_{\underline{\underline{s}}}^{\underline{\underline{\Theta}}_s}$. Substituting $\underline{\underline{\Theta}}_s = \frac{k}{m_s}\hat{T}\underline{\underline{I}}$ into Eq. (34) leads to the known expression for G_s (Eq. (8)).
The equality $H(G_s) = H(f_s^{LocM})$ is inspected by comparing the difference in the entropy expression in Eq. (36) and holds only if $n\hat{T} = \sum_{s=1}^{2} n_s T_s$. Substituting this into Eq. (26), it follows that $u_s = u_0$, which leads to $u_s = u_0 = u_s^{(g)}$ and $\hat{T} = T$. Under these constrains the distribution function G_s is equivalent to the isotropic Maxwellian or $G_s \equiv f_s^M$ and $H(G_s) = H(f_s^M) = H(f_s^{LocM})$.

$$\frac{\partial H}{\partial t} = 0 \Longleftrightarrow G_s^{ES} = f_s^M \tag{39}$$

Therefore the equality of the H-functional is achieved at equilibrium and both species have a Maxwellian isotropic distribution. The species target equilibrium temperature and velocities are equal to the mean properties of the mixture.

6.3 Indifferentiability principle

The indifferentiability principle, described by Garzo et al.[16], requires the ES-BGK model for species to reduce to a single species ES-BGK model when the species are identical. To test this principle the species masses are set equal (for a binary mixture this means $m_1 = m_2$) and the distribution function: $\mathbf{G} = \sum_{s=1}^{2} G_s^{ES}$ should satisfy the ES monospecies kinetic model. A necessary assumption [8] is that $u_s = u_0$ for all species s, which leads to $u_s^{(g)} = u_0$ and $\hat{T} = T$. With equal species mass and velocity, the distribution functions differ only by number density n_s and can easily be added up to the distribution function $\mathbf{G}(n, m, u_0, \hat{T})$, which satisfies the indifferentiability principle. Note that under these conditions the principle is also valid for the Shakhov-based model.

7 Continuum Limit

In this section the continuum limit of the mass, momentum and energy equations is examined and Groppi et al.'s, Shakhov-based and ES-based models are compared using the Chapman-Enskog expansion. This is performed in order to achieve the asymptotic limit, but also to emphasize the difference between the models and how and where the two proposed models make corrections. In the near-continuum regime, the Knudsen number can be used as a small perturbation parameter $\epsilon \ll 1$ to perform a Chapman Enskog expansion up to $O(\epsilon^2)$ order.

$$\epsilon\Big(\frac{\partial f_s^\epsilon}{\partial t} + \underline{u}\cdot\nabla_{\underline{x}} f_s^\epsilon\Big) = \nu\Big(F_s\big[f_1^\epsilon, f_2^\epsilon\big] - f_s^\epsilon\Big) \quad ; \quad s = 1,2 \tag{40}$$

where F_s=G_s, G_s^{Sh}, G_s^{ES} for the corresponding model, $\nu = \frac{\nu}{1-\nu_{ES}}$ for the ES model and f_s^ϵ is expanded in powers of ϵ. At zeroth order $F_s\big[f_1^0, f_2^0\big] = f_s^M$, as given by Eq. (6) and expressing the non-equilibrium distribution function from Eq. (40) leads to:

$$f_s^\epsilon(\underline{u}) = F_s\big[f_1^\epsilon, f_2^\epsilon\big](\underline{u}) - \frac{\epsilon}{\nu}\Big(\frac{\partial f_s^M}{\partial t} + \underline{u}\cdot\nabla_{\underline{x}} f_s^M\Big) + O(\epsilon^2) \tag{41}$$

For simplicity the one-dimensional model is considered from here onwards. The evolution of the Maxwellian distribution can be derived and after substituting the time derivatives with the spatial gradients from the unexpanded conserved moments leads to:

$$\begin{aligned}
&\frac{\partial f_s^M}{\partial t} + u\frac{\partial f_s^M}{\partial x} = f_s^M\Bigg[\frac{1}{n_s}\big(u-u_0\big)\Big\{\frac{\partial n_s}{\partial x} - \frac{\rho_s}{\rho}\frac{\partial n}{\partial x}\Big\} \\
&+\Big(m_s\frac{\big(u-u_0\big)^2 + v^2 + w^2}{2kT^2} - \frac{m_s n}{\rho T} - \frac{3}{2T}\Big)\Big\{\big(u-u_0\big)\frac{\partial T}{\partial x}\Big\} \\
&+\frac{m_s\big(u-u_0\big)}{kT}\Big\{\big(u-u_0\big)\frac{\partial u_0}{\partial x}\Big\} - \Big(m_s\frac{\big(u-u_0\big)^2 + v^2 + w^2}{3kT}\Big)\Big(\frac{\partial u_0}{\partial x}\Big)\Bigg]
\end{aligned} \tag{42}$$

A key aspect of the kinetic model for the binary mixture is the velocity drift of the species relative to the mean gas mixture. For the velocity component in $x-$direction, the following moments involving molecular velocity u in $x-$direction can be used,where as before F_s=G_s, G_s^{Sh}, G_s^{ES} for the corresponding model, $\nu = \frac{\nu}{1-\nu_{ES}}$ for the ES model.

$$n_s u_s^\epsilon = \iiint_{-\infty}^{\infty} u\Big[F_s - \frac{\epsilon}{\nu}\Big(\frac{\partial f_s^M}{\partial t} + u\frac{\partial f_s^M}{\partial x}\Big)\Big]d\underline{u} = n_s u_s^{(g)} - \frac{kT\epsilon}{\nu}\Big[\frac{1}{m_s}\frac{\partial n_s}{\partial x} - \frac{n_s}{\rho}\frac{\partial n}{\partial x} + \frac{n_s}{T}\Big(\frac{1}{m_s} - \frac{n}{\rho}\Big)\frac{\partial T}{\partial x}\Big] \tag{43}$$

Inserting the expression for $u_s^{(g)}$ for each model, the species velocity in the $x-$ direction up to 1st-order in ϵ is:

$$u_s^{\epsilon} = u_0 - \frac{\epsilon kT}{n_s \eta}\Big[\frac{1}{m_s}\frac{\partial n_s}{\partial x} - \frac{n_s}{\rho}\frac{\partial n}{\partial x} + \frac{n_s}{T}\Big(\frac{1}{m_s} - \frac{n}{\rho}\Big)\frac{\partial T}{\partial x}\Big] \tag{44}$$

Total mass, momentum and energy of the system need to be conserved. The mass and momentum equations for the three models in the continuum limit up to $O(\epsilon^2)$ order are recovered (Eq. (45) and (46)), after substituting the expression for $u_s^{(g)}$,$\hat{T}$ and for the ES-based model - the matrix elements λ_s as described in more detail in Appendix-CE limit. Mass conservation equation:

$$\frac{\partial n_s}{\partial t} + \frac{\partial}{\partial x}\Big\{n_s u_0 - \epsilon\frac{kT}{\eta}\Big[\frac{1}{m_s}\frac{\partial n_s}{\partial x} - \frac{n_s}{\rho}\frac{\partial n}{\partial x} + \frac{n_s}{T}\Big(\frac{1}{m_s} - \frac{n}{\rho}\Big)\frac{\partial T}{\partial x}\Big]\Big\} = 0 \tag{45}$$

From the Chapman-Enskog expansion we find for the mixture momentum equation:

$$\frac{\partial \rho u_0}{\partial t} + \frac{\partial}{\partial x}\Big\{nkT + \rho u_0^2 - \frac{\epsilon}{\nu}nkT\frac{4}{3}\frac{\partial u_0}{\partial x}\Big\} = 0$$

The momentum equation in the Navier-Stokes equations for a compressible one-dimensional flow is most commonly expressed as:

$$\frac{\partial \rho u_0}{\partial t} + \frac{\partial}{\partial x}\Big\{nkT + \rho u_0^2 - \mu\frac{4}{3}\frac{\partial u_0}{\partial x}\Big\} = 0 \tag{46}$$

From which it follows that the viscosity coefficient $\mu = \frac{\epsilon}{\nu}nkT$ as the expected expression in front of the velocity derivative in the momentum flux.

The corrections in the new models affect the limit of the energy equation and the following three equations demonstrate the introduced change, found in the underbraced temperature gradient term. Since $Pr = \frac{1}{1-\nu_{ES}}$ [3], the Shakhov and ES corrections lead to the same expression for the energy equation. Moreover, when $Pr = 1$ or $\nu_{ES} = 0$ the limit reduces to the original model. This is a desired result and shows theoretical consistency between all models. Note that by examining problems with $Pr = 1$ and $\nu_{ES} = 0$, numerical consistency will also be demonstrated. For the Groppi et al's model the energy equation is:

$$\begin{aligned}\frac{\partial}{\partial t}\Big[\frac{3}{2}nkT + \frac{1}{2}\rho_0 u_0^2\Big] + \frac{\partial}{\partial x}\Bigg\{\sum_{s=1}^{2} m_s n_s\Big[\frac{5}{2}\frac{kT}{m_s}u_0 + \frac{1}{2}u_0^3 + \Big\{\frac{5}{2}\frac{kT}{m_s} + \frac{3}{2}u_0^2\Big\}(u_0 - u_s)\Big] \\ -\epsilon\frac{kT}{\nu}\sum_{s=1}^{2}\Big[\frac{4}{3}n_s u_0\frac{\partial u_0}{\partial x} + \underbrace{\frac{5}{2}n_s\Big(\frac{k}{m_s}\Big)\frac{\partial T}{\partial x}}\Big]\Bigg\} = 0\end{aligned} \tag{47}$$

The Shakhov correction shows a dependency on Pr :

$$\frac{\partial}{\partial t}\Big[\frac{3}{2}nkT+\frac{1}{2}\rho_0 u_0^2\Big]+\frac{\partial}{\partial x}\Bigg\{\sum_{s=1}^{2}m_s n_s\Big[\frac{5}{2}\frac{kT}{m_s}u_0+\frac{1}{2}u_0^3+\Big\{\frac{5}{2}\frac{kT}{m_s}+\frac{3}{2}u_0^2\Big\}\big(u_0-u_s\big)\Big] \\ -\epsilon\frac{kT}{\nu}\sum_{s=1}^{2}\Big[\frac{4}{3}n_s u_0\frac{\partial u_0}{\partial x}+\underbrace{\frac{1}{Pr}\frac{5}{2}n_s\Big(\frac{k}{m_s}\Big)\frac{\partial T}{\partial x}}\Big]\Bigg\}=0 \tag{48}$$

The ES-based model energy equation:

$$\frac{\partial}{\partial t}\Big[\frac{3}{2}nkT+\frac{1}{2}\rho_0 u_0^2\Big]+\frac{\partial}{\partial x}\Bigg\{\sum_{s=1}^{2}m_s n_s\Big[\frac{5}{2}\frac{kT}{m_s}u_0+\frac{1}{2}u_0^3+\Big\{\frac{5}{2}\frac{kT}{m_s}+\frac{3}{2}u_0^2\Big\}\big(u_0-u_s\big)\Big] \\ -\epsilon\frac{kT}{\nu}\sum_{s=1}^{2}\Big[\frac{4}{3}n_s u_0\frac{\partial u_0}{\partial x}+\underbrace{(1-\nu_{ES})\frac{5}{2}n_s\Big(\frac{k}{m_s}\Big)\frac{\partial T}{\partial x}}\Big]\Bigg\}=0 \tag{49}$$

8 Transport properties

To define the transport coefficients the flux vectors in the hydrodynamic limit of the kinetic equations need to be studied. It should be noted that the same assumption as for the Boltzmann equation is made and the gas is considered with low enough density so that the three-body collisions can be ignored.

8.1 Diffusion

The mass flux vector in the species conservation equations, excluding the external forces, is caused by gradients of concentration, pressure and temperature and has the following form for species s [25]:

$$\underline{j}_s=n_s m_s\overline{\underline{V}}_s=\frac{n^2}{\rho}m_s m_r\mathcal{D}_{sr}\underline{d}_r-D_s^T\frac{\partial\, lnT}{\partial x} \tag{50}$$

where $\mathcal{D}_{sr}=\mathcal{D}_{rs}$ is the binary diffusion coefficient and is single valued, $r\in\{1,2\}$ and $r\neq s$, $\underline{d}_r$ is such that:

$$\underline{d}_r=\frac{\partial}{\partial\underline{x}}\Big(\frac{n_r}{n}\Big)+\Big(\frac{n_r}{n}-\frac{n_r m_r}{\rho}\Big)\frac{\partial\, lnp}{\partial\underline{x}} \tag{51}$$

Splitting the pressure gradient into concentration and temperature expressions and considering only the ordinary diffusion part, provides an expression for the mass heat flux based on the binary diffusion coefficient $\mathcal{D}_{sr}$.

$$\underline{j}_s=-\frac{n}{\rho}m_s m_r\mathcal{D}_{sr}\Big(\frac{\partial n_s}{\partial\underline{x}}-\frac{\rho_s}{\rho}\frac{\partial n}{\partial\underline{x}}\Big) \tag{52}$$

The binary diffusion coefficient is expressed from the comparison between the mass heat flux from the CE expansion from Eq. (44) and the above expression leads to:

$$\mathcal{D}_{sr} = \frac{\epsilon k T \rho}{\eta n m_s m_r} \tag{53}$$

8.2 Viscosity

The viscosity coefficient for the mixture is shown in Section 7 (Eq. (46)) to be in the form:

$$\mu = \frac{\epsilon}{\nu} n k T \tag{54}$$

For a binary mixture the diffusion and viscosity coefficients are closely connected [25]:

$$\mu = \frac{5}{3} \frac{m_1 m_2}{(m_1 + m_2)} \frac{n \mathcal{D}_{12}}{A_{12}^*} \tag{55}$$

where A_{12}^* is a non-dimensional coefficient, defined by the ratio of collision integrals and is in general a function of the gas temperature and the force law between molecules. However, the variation of A_{12}^* is limited and after inspection of the values of noble mixtures presented in the Weissmann and Mason paper [38], a good approximation for A_{12}^* is $A_{12}^* = 1.11$. Now there is a platform to express the relaxation ratio $\frac{\eta}{\nu}$, required for the computation of the species target velocity $u_s^{(g)}$ and the modified temperature $\hat{T}$.

$$\frac{\eta}{\nu} = \frac{5}{3} \frac{1}{(m_1 + m_2) A_{12}^*} \frac{\rho}{n} \tag{56}$$

It is clear that the relaxation fraction will vary only in the regions where strong non-equilibrium effects and large gradients occur and this effect will be amplified for higher mass ratios.

8.3 Heat Flux

The model introduced by Groppi et al. [19] can recover correctly the diffusion and the viscous coefficients due to the introduction of a second relaxation parameter. The velocity equalizer coefficient η and together with the standard BGK relaxation coefficient ν allows for a maximum of two transport coefficients to be set. The Shakhov and ES-based extensions of this model instigate a third variable- the Prandtl number Pr and the corresponding anisotropic model variable - ν_{ES}. The goal is to recover the thermal conductivity and have a system with three correct transport coefficients. We inspect the thermal conductivity k_s in the expression for the heat flux, found by a standard integration

with respect to the mean gas mixture velocity u_0. The non-equilibrium part is common for all models and yields:

$$\iiint_{-\infty}^{\infty} m_s(\underline{u}-\underline{u}_0)\frac{1}{2}\big((\underline{u}-\underline{u}_0)^2\big)\Big\{-\frac{\epsilon}{\nu}\Big(\frac{\partial f_s^M}{\partial t}+\underline{u}\frac{\partial f_s^M}{\partial \underline{x}}\Big)\Big\}d\underline{u}=\frac{\eta}{\nu}\frac{5}{2}n_skT(\underline{u}_s-\underline{u}_0)-\frac{\epsilon}{\nu}\frac{5}{2}k\frac{n_skT}{m_s}\frac{\partial T}{\partial \underline{x}}+O(\epsilon^2) \tag{57}$$

where as before, for the ES-based model in the above expression $\nu=\frac{\nu}{1-\nu_{ES}}$. The moments with respect to the equilibrium distribution functions are expressed as:

$$\iiint_{-\infty}^{\infty} m_s(\underline{u}-\underline{u}_0)\frac{1}{2}\big((\underline{u}-\underline{u}_0)^2\big)G_s^{Sh}=\Big(1-\frac{\eta}{\nu}\Big)\frac{5}{2}n_skT(\underline{u}_s-\underline{u}_0)+(1-Pr)\underline{q}_s^{corr}+O(\epsilon^2) \tag{58}$$

$$\iiint_{-\infty}^{\infty} m_s(\underline{u}-\underline{u}_0)\frac{1}{2}\big((\underline{u}-\underline{u}_0)^2\big)G_s^{ES}=\Big(1-\frac{\eta}{\nu}(1-\nu_{ES})\Big)(\underline{u}_s-\underline{u}_0)\Big(\frac{5}{2}n_skT-\nu_{ES}\frac{\epsilon}{\nu}n_skT\frac{4}{3}\frac{\partial u_0}{\partial x}\Big)+O(\epsilon^2) \tag{59}$$

Combining the moment of the Shakhov and ES-based model with the corresponding CE expansion, provides the heat flux q_s for each model.

$$\begin{aligned}\underline{q}_s^{Sh}&=\frac{5}{2}n_skT(\underline{u}_s-\underline{u}_0)-\frac{\epsilon}{\nu}\frac{5}{2}k\frac{n_skT}{m_s}\frac{\partial T}{\partial \underline{x}}+(1-Pr)\underline{q}_s^{corr}+O(\epsilon^2)\\ \underline{q}_s^{ES}&=\frac{5}{2}n_skT(\underline{u}_s-\underline{u}_0)-\frac{\epsilon(1-\nu_{ES})}{\nu}\frac{5}{2}k\frac{n_skT}{m_s}\frac{\partial T}{\partial \underline{x}}+O(\epsilon^2)\end{aligned} \tag{60}$$

Substituting the previously derived expression for $\underline{q}_s^{corr}$ - Eq. (15) for the Shakhov model:

$$\underline{q}_s^{Sh}=\frac{5}{2}n_skT(\underline{u}_s-\underline{u}_0)-\frac{\epsilon}{\nu}\frac{5}{2}\frac{k}{Pr}\frac{n_skT}{m_s}\frac{\partial T}{\partial \underline{x}}+O(\epsilon^2) \tag{61}$$

Again, we observe consistency between the models when $(1-\nu_{ES})=1/Pr$. The species heat flux is determined by the combination of Fourier law (term involving the temperature gradient) and Dufour effect (term based on the diffusion effect). It is important to remember that only the mixture energy is conserved, while species energy equations would contain a source term due to the exchange of energy between the species. This also means that in classical fluid dynamics at Navier-Stokes level the heat flux of the system is the summation of the heat flux contribution of each species. Note that if the species have the same mass, the difference between $\underline{u}_s$ and $\underline{u}_0$ will vanish and the Dufour effect will not contribute to the heat flux.

The main advantage of the proposed models lies in the definition of the Fourier part of the heat flux. The thermal conductivity is qualitatively and quantitatively reproduced and the thermal conductivity coefficient κ_s is recovered

for both models as:

$$\kappa_s = \frac{\epsilon}{\nu}\frac{5}{2}\frac{k}{Pr}\frac{n_s kT}{m_s} = \frac{\epsilon(1-\nu_{ES})}{\nu}\frac{5}{2}k\frac{n_s kT}{m_s} \tag{62}$$

The Prandtl number for a gas mixture Pr_{mix} is evaluated from the gas mixture properties as: $Pr_{mix} = c_p\mu/\kappa$, where $c_p = \frac{5}{2}\frac{k}{m}$ is evaluated with the mixture mass $m = \rho/n$, μ is the mixture viscosity (Eq. 54) and κ is the mixture thermal conductivity coefficient in front of the temperature gradient, received from summing the heat flux expressions (Eq. 60 for the ES-based model and Eq. 61 for the Shakhov-based model) over all species s.

$$Pr_{mix} = \frac{c_p\mu}{\kappa} = \frac{\frac{5}{2}\frac{k}{m}\frac{\epsilon}{\nu}nkT}{\frac{\epsilon}{\nu}\frac{5}{2}\frac{k}{Pr}kT\sum_s\frac{n_s}{m_s}} = \frac{Pr}{\sum_s\frac{n_s}{n}\frac{m}{m_s}} \tag{63}$$

where $Pr = 1/(1-\nu_{ES})$ for the ES-based model. The Prandtl number for a gas mixture is known to vary with the mass and concentration of each species and the same conclusion is observed in the expression for the Pr_{mix}. The maximum value of Pr_{mix} is found in the limiting case when the gas mixture reduces to a pure gas and $Pr_{mix} = Pr$.

9 Methodology

The two newly derived models are now evaluated and compared. The structure of a normal shock wave is investigated. This is the simplest problem that involves strong gradients and non-equilibrium flow and is also investigated extensively - experimentally e.g. [12] [23] and numerically, e.g.[30], providing a dataset for validation. The models are inspected under different free-stream conditions and validated against the results obtained for the full Boltzmann model, available in the literature [30]. The kinetic models are implemented with the discrete velocity method (DVM) [32]. DVM is accurate and reliable numerical approach and allows for strong non-equilibrium flows.

9.1 The problem

A steady flow of a binary mixture (species 1- light gas and 2- heavy gas) going through a normal shock wave is considered. The x-axis denotes the physical space, where far upstream and far downstream from the shock the mixture is in two different equilibrium states, defined by the species number density n_s,velocity u_s and temperature T_s. Note that in equilibrium the gas mean and species mean velocities are equal $u_1 = u_2 = u_0$, as are the temperatures $T_1 = T_2 = T$ in each state. The state to state change of the flow variables across the shock in the initial solution is set by the Rankine-Hugoniot relationship, which depends on the free-stream Mach number M_∞. Note that the free-stream Mach number is defined with the mixture speed of sound a_{mix}. Therefore $M_\infty = u_0/a_{mix}$ with $a_{mix} = \sqrt{\gamma kT/m_{mix}} = \sqrt{\gamma kTn/\rho}$, where m_{mix} is the mass of the mixture defined by the mixture density ρ divided by the

mixture number density n. To define a specific problem, the free-stream Mach number, species concentration and the mass ratio are assigned.

9.2 Numerical method

Numerical application of the described kinetic models is performed by the standard approach of the discrete velocity method (DVM) [32]. Possible molecular velocities are uniformly spaced in a defined velocity domain. For a one-dimensional normal shock wave problem a hundred discrete velocities are sufficient and have been used in all simulations. The distribution function and the fluxes are evaluated for each of the velocities in every cell. The moments of the distribution functions (macroscopic variables) are found applying the trapezoidal rule. A finite-volume scheme and a second order TVD time marching method [24][15] are used to numerically discretise the models' governing equation. Note that in contrast to a continuum solver, which stores only the macroscopic variables in each cell, the two kinetic solvers based on the DVM require much more computational time and memory. For two- and three-dimensional cases code parallelization is necessary for most cases of interest.

9.3 Dimensional reduction

In the one-dimensional formulation, the equilibrium functions are dimensionally reduced to quasi-one-dimensional functions to reduce computational cost. Since the mean velocities v_0, w_0 in the y and z-directions are zero, the species distribution function f_s reduces to to translational g_s and thermal h_s energy component - Eq. (64). The macroscopic variables are then found by taking moments of the reduced distribution functions.

$$
\begin{aligned}
g_s &= \iint_{-\infty}^{\infty} f_s \; dvdw \\
h_s &= \iint_{-\infty}^{\infty} (v^2 + w^2) f_s \; dvdw
\end{aligned}
\tag{64}
$$

Therefore the solver uses four velocity distribution functions- two for each species- to solve the flowfield.

9.4 Dimensionless form

The macroscopic variables are non-dimensionalized and the reference values are described in this subsection. The lighter species and its mass m_1 are taken as reference. All velocities are non-dimensionalized with the most probable speed u_r of the light species. Elements of the anisotropic tensor for the ES-based model λ_r^s are scaled per species to preserve the scaling for the distribution functions as in the Shakhov-based model - f_r, g_r, h_r. The constant $\beta = m_2/m_1$

is the mass ratio in the expressions for the distribution functions of the heavy gas.

$$
\begin{aligned}
u_r &= \sqrt{2kT_r/m_1} \\
\rho_r &= n_r m_1 \\
\lambda_r^s &= R_s T_r = \frac{kT_r}{m_s} \\
f_r &= \frac{n_r}{u_r^3} = \frac{n_r}{\left(2kT_r/m_1\right)^{3/2}} \\
g_r &= \frac{n_r}{u_r} = \frac{n_r}{\sqrt{2kT_r/m_1}} \\
h_r &= n_r u_r = n_r\sqrt{2kT_r/m_1} \\
\beta &= m_2/m_1 \\
\lambda_{ref} &= \frac{1}{\sqrt{2}\pi d_1^2 n} \\
L_{ref} &= \frac{u_{ref}}{t_{ref}} = \frac{u_{ref}}{\tau_{ref}} = \frac{u_{ref}\mu_{ref}}{p_{ref}}
\end{aligned}
\tag{65}
$$

In the kinetic model, the reference length L_{ref} is defined by reference time and velocity, where the $t_{ref} = \tau_{ref}$ - the collision rate, expressed from the mixture pressure and viscosity. The reference viscosity is taken for a smooth, rigid, elastic sphere [13] and defined with diameter d_1 and mass of the mixture $m_{mix} = \rho/n$ to allow for a comparison the Boltzmann solution [30] with the mean free path λ_{ref} as a reference length.

$$
\mu_{ref} = \frac{5}{16d_1^2}\sqrt{\frac{km_{mix}T}{\pi}} \tag{66}
$$

The resultant reference length:

$$
L_{ref} = \frac{\sqrt{\frac{2kT}{m_1}}\frac{5}{16d_1^2}\sqrt{\frac{km_{mix}T}{\pi}}}{nkT} = \frac{5\sqrt{2}}{16\sqrt{\pi}d_1^2 n}\sqrt{\frac{m_{mix}}{m_1}} = \frac{5\sqrt{2}}{16\sqrt{\pi}d_1^2 n}\sqrt{\frac{n_1m_1 + n_2m_2}{m_1(n_1+n_2)}} \tag{67}
$$

The ratio of the two reference lengths is the required scaling factor with all variables taken at free-stream conditions.

$$
\frac{L_{ref}}{\lambda_{ref}} = \frac{5\sqrt{\pi}}{8}\sqrt{\frac{n_1 + \beta n_2}{n_1 + n_2}} \tag{68}
$$

9.5 Normalized Values

The macroscopic quantities presented in this part are normalized following Kosuge's approach [30], where y is the macroscopic variable, Y_- is the pre-shock value of y and Y_+ is post-shock:

$$\tilde{y} = \frac{y - Y_-}{Y_+ - Y_-} \tag{69}$$

Note that the tilde is omitted from here on for simplicity. Also, the origin of the plots ($X = 0$) is where the total number density is half of the sum of the species number densities.

10 Validation

The profile of a normal shock wave is studied for a binary mixture of gases with different mass and with mean species velocities and temperatures that are allowed to deviate. The goal is to inspect the effect of different free stream conditions (Mach number, ratio of masses and concentration ratio) on the distribution of the macroscopic species variables and validate the model for variety of conditions. Test case conditions are summarized in Table 1.

M_∞	m_2/m_1	n_1/n
1.5	2	0.9
1.5	4	0.9
1.5	2	0.5
3	2	0.9
3	2	0.5

Table 1: Test Case Conditions for Normal Shock Wave

Figures 1 and 2 show the normalized number density and temperature for each species through the shock profile under the specified conditions. Figures 1 (a) and (c) focus on comparing the Shakhov and ES-based models with Kosuge's full Boltzmann model for two different free-stream Mach numbers $M_\infty = 1.5, 3$. Combining the higher velocities with a gas having predominantly the light component leads to an overshoot of the heavy species' temperature, which is a known numerical result [6]. The approximate models follow closely the full model and match well with each other. For normal shocks at higher Mach numbers, longer upstream tails for the species temperatures are observed. This is a known disadvantage of all BGK-type models and the introduced corrections in the two kinetic models cannot target this drawback. This result is also observed for the uncorrected model on figure 1 (b) and (d). Comparing the results of the two new models, we can see that the upstream tail is more pronounced in the ES model than in the Shakhov-based model, consistent with observations for single-species simulations based on ES and Shakhov models[14]. The Shakhov model with Prandtl number 1 eliminates the introduced correction (Fig. 1 (b)) and the same happens

when the ES-based model is simulated with $\nu_{ES} = 0$ (Fig. 1 (d)). The original model follows the results of the full Boltzmann equation, but clearly reveals the changes the new models introduce. The difference is emphasized for more extremely conditions. For higher Mach number (Fig. 1 (c) and (d)) Groppi et al.'s model moves further away from the target solution, while the Shakhov- and ES-based models preserve the structure of the shock wave more closely.

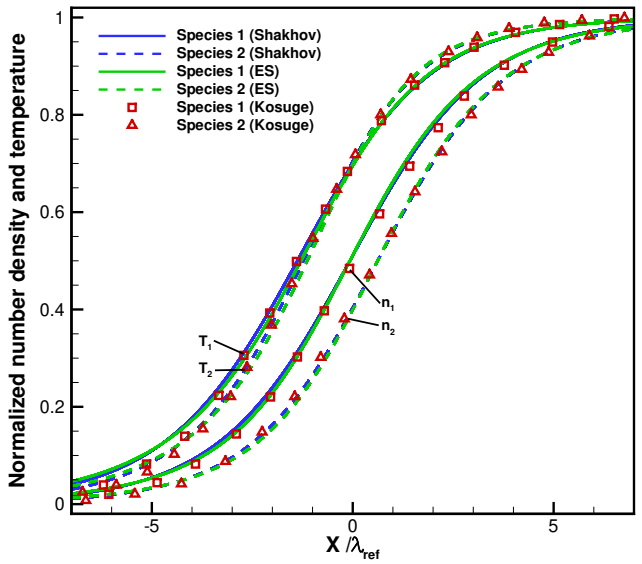

(a) $M = 1.5;\ m_2/m_1 = 2;\ n_1/n = 0.9$

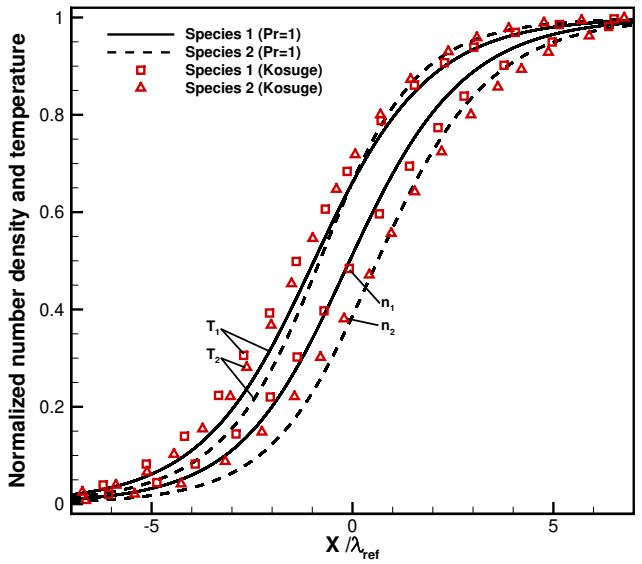

(b) $M = 1.5;\ m_2/m_1 = 2;\ n_1/n = 0.9;\ Pr = 1$

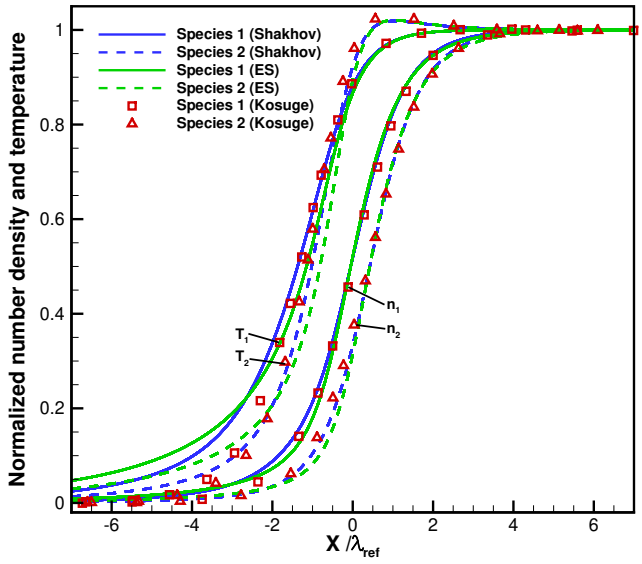

(c) $M = 3;\ m_2/m_1 = 2;\ n_1/n = 0.9$

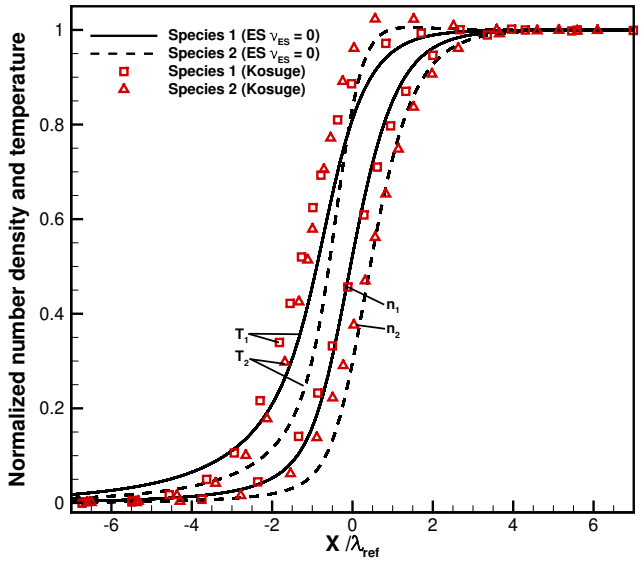

(d) $M = 3;\ m_2/m_1 = 2;\ n_1/n = 0.9;\ \nu_{ES} = 0$

Figure 1: Validation and comparison of the Shakhov and ES-based models with Kosuge's full Boltzmann model [30] and without the added corrections for flow conditions: (a) $M = 1.5;\ m_2/m_1 = 2;\ n_1/n = 0.9$ (b) $M = 1.5;\ m_2/m_1 = 2;\ n_1/n = 0.9;\ Pr = 1$. (c) $M = 3;\ m_2/m_1 = 2;\ n_1/n = 0.9$ (d) $M = 3;\ m_2/m_1 = 2;\ n_1/n = 0.9;\ \nu_{ES} = 0$.

Further validation and parametric study show the change of the flow with the increase of the mass ratio from 2 to 4

on figure 2 (a). The shock thickness increases and the shock front is more gradual. The solutions demonstrate that

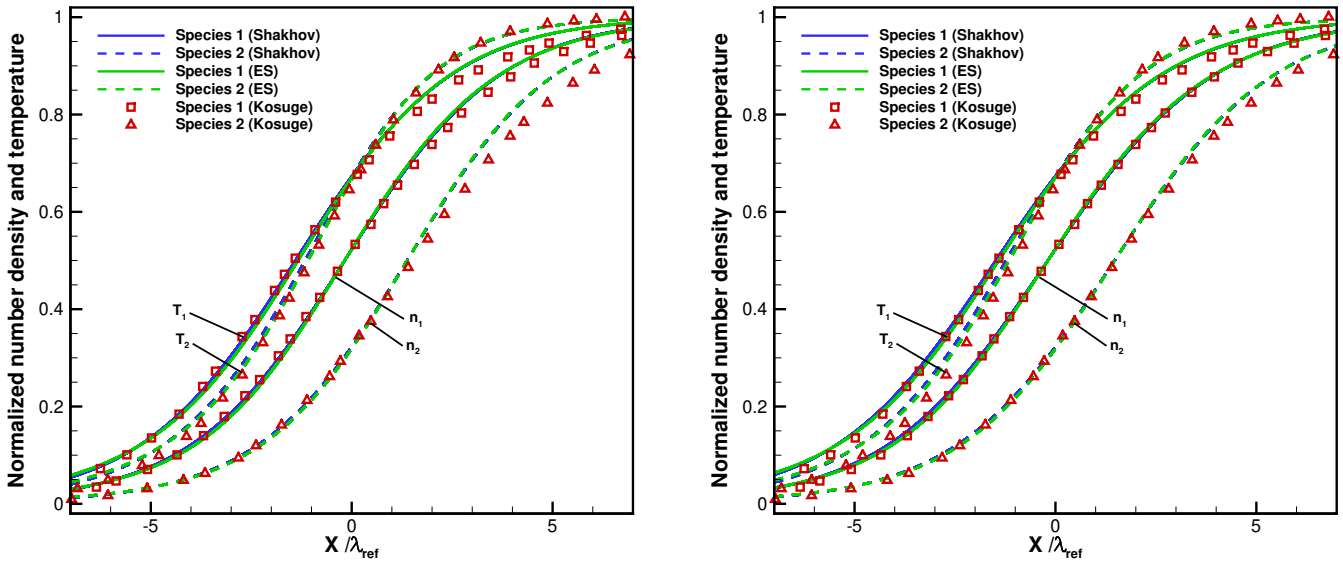

(a) $M = 1.5;\ m_2/m_1 = 4;\ n_1/n = 0.9$

(b) $M = 1.5;\ m_2/m_1 = 4;\ n_1/n = 0.9;\ \omega = 0.72$

(c) $M = 1.5;\ m_2/m_1 = 2;\ n_1/n = 0.5$

(d) $M = 3;\ m_2/m_1 = 2;\ n_1/n = 0.5$

Figure 2: Validation of the Shakhov and ES-based models with Kosuge's full Boltzmann model [30] for flow conditions: (a) $M = 1.5;\ m_2/m_1 = 4;\ n_1/n = 0.9$ (b) $M = 1.5;\ m_2/m_1 = 4;\ n_1/n = 0.9;\ \omega = 0.72$. (c) $M = 1.5;\ m_2/m_1 = 2;\ n_1/n = 0.5$ (d) $M = 3;\ m_2/m_1 = 2;\ n_1/n = 0.5$.

the lighter the species becomes in comparison to the other gas, the further upstream changes in the flow are observed. This phenomena has previously been confirmed for monoatomic and diatomic gas mixtures with the generalized Boltzmann equation [39].

All simulations until now were performed for a hard sphere model in order to compare with the Boltzmann solution.

The effect of molecular model is inspected by comparing at the same free-stream conditions and changing the viscosity power law - see figures 2 (a)-hard-sphere model ($\omega = 0.5$) with (b)-variable hard-sphere model ($\omega = 0.72$). The changes are significantly small in comparison to the change introduced by the Prandtl number correction, which is the desired result.

Two more cases with 50% concentration for each component and mass ratio of 2, but under different Mach numbers ($M_\infty = 1.5, 3$) allow to solely examine the effect of the ratio of light to heavy species in the flow (Fig. 2 (c) and (d)). The figures show that the shock thickness reduces with the increase of heavy species in the flow and the structure becomes steeper overall, which corresponds to the properties of the heavy species observed until now.

Note that for any pure monoatomic gas the Prandtl number is 2/3, while it is known that for a binary mixture of monoatomic gases it is reduced, according to the mass ratio and concentration [35] [18]. For 90% concentration of the lighter species, the mixture Prandtl number remains close to the target Prandtl number (Pr = 2/3), i.e. the resultant mixture Prandtl number is $Pr_{mix} = 0.638$, however for $n_1/n = 50\%$ and $\beta = 2$ it reduces to $Pr_{mix} = 0.593$. Increasing the mass ratio to $\beta = 10$, e.g. for a helium-argon mixture can decrease the mixture Prandtl number to ≈ 0.22 , making the Shakhov and ES-based corrections further pronounced.

Characteristic features of the problem are observed, including the lighter species (species 1) reacting faster to the shock, while the temperature rise of the heavy species T_2 is steeper and crosses T_1. Species mean velocities and number densities also react at different rate but unlike the temperatures do not intersect at any point. Based on the validation and parametric study shown, a good agreement with the results by Kosuge et al. [30] is evident. Note that the findings in this section are verified with the more detailed results of the full Boltzmann model and are consistent with the trends of other BGK-based models [37] [43]. From the results for the normal shock waves, the Shakhov-based model shows a slightly better behavior upstream of the shock wave in comparison to the ES-based model. Given the fact that the numerical complexity for this model is also lower, this model is the preferred choice for normal shock wave simulations. The relative merit for both models will be further assessed for a wider range of test cases in future studies.

11 Conclusion

Two newly introduced kinetic models for a binary monoatomic gas mixture with separate species mean velocities and temperatures are presented. The models improve upon an established relaxation model with corrections in the distribution function consistent with extensions of single species models. In the literature there are models with a maximum of two correct transport coefficients. The key novelty of both models is the recovery of three coefficients, affecting the diffusion, viscosity and heat flux of the flow. Important features of the Boltzmann equation are preserved- e.g. non-negativity of density and temperature fields, conservation laws, indifferentiability principle.

The Chapman-Enskog expansion is used to derive the hydrodynamic limit and details of the transport properties. For the ES-based model the H-theorem and collision equilibria are shown. Moreover, the models are validated numerically by investigating the structure of a normal shock wave against the benchmark results of the full Boltzmann equation. The results agree well and the influence of the correct Prandtl number is evident. For the considered test cases, involving normal shocks, the Shakhov-based model showed a slightly better results, particularly upstream of the shock. The lower computational complexity of this model is a further benefit. Future studies involving a wider range of test cases will further assess the relative merits of the ES- and Shakhov-based models in terms of physical accuracy. This work will allow for more accurate modelling of rarefied and high-speed flows, where the heat flux has significant impact on the system. The models can be improved upon by incorporating the correct Soret and Dufour coefficients. This forms part of the future work as well as testing more complex geometries, higher mass ratios and an extension to diatomic gas mixtures.

Acknowledgments

The authors would like to acknowledge the financial support provided by the University of Glasgow. Results were obtained using the EPSRC funded ARCHIE-WeSt High Performance Computer (www.archie-west.ac.uk). EPSRC grant no. EP/K000586/1.

Appendix A: Shakhov-based model

Moments of the quasi one-dimensional Shakhov-based models are detailed:

$$\iiint_{-\infty}^{\infty} G_s^{Sh} d\underline{u} = n_s \quad ; \quad \iiint_{-\infty}^{\infty} \underline{u} G_s^{Sh} d\underline{u} = n_s \underline{u}_s^{(g)}$$

$$\iiint_{-\infty}^{\infty} u^2 G_s^{Sh} d\underline{u} = n_s\Big(\frac{k\hat{T}}{m_s}\Big) + n_s (u_s^{(g)})^2 \quad ; \quad \iiint_{-\infty}^{\infty} v^2 G_s^{Sh} d\underline{u} = \iiint_{-\infty}^{\infty} w^2 G_s^{Sh} d\underline{u} = n_s\Big(\frac{k\hat{T}}{m_s}\Big)$$

$$\iiint_{-\infty}^{\infty} u^3 G_s^{Sh} d\underline{u} = 3 n_s u_s^{(g)} \Big(\frac{k\hat{T}}{m_s}\Big) + n_s (u_s^{(g)})^3 + \frac{6\big(1-Pr\big) q_{x_s}^{corr}}{5 m_s}$$

$$\iiint_{-\infty}^{\infty} u v^2 G_s^{Sh} d\underline{u} = \iiint_{-\infty}^{\infty} u w^2 G_s^{Sh} d\underline{u} = n_s u_s^{(g)} \Big(\frac{k\hat{T}}{m_s}\Big) + \frac{2\big(1-Pr\big) q_{x_s}^{corr}}{5 m_s}$$

Appendix B: Tensor elements of the ES-based model

For a quasi one-dimensional flow ($u_0 \neq 0, v_0 = 0, w_0 = 0$) the elements of the matrix $\mathbf{\Lambda}_s$ can be obtained as:

$$\lambda_{11}^s = \big(1-\nu_{ES}\big)\Big(\frac{k\hat{T}}{m_s}\Big) + \frac{\nu_{ES}}{n_s}\iiint_{-\infty}^{\infty}\big(u-u_s^{(g)}\big)^2 f_s d\underline{u}$$

$$\lambda_{22}^s = \big(1-\nu_{ES}\big)\Big(\frac{k\hat{T}}{m_s}\Big) + \frac{\nu_{ES}}{n_s}\iiint_{-\infty}^{\infty} v^2 f_s d\underline{u}$$

$$\lambda_{33}^s = \big(1-\nu_{ES}\big)\Big(\frac{k\hat{T}}{m_s}\Big) + \frac{\nu_{ES}}{n_s}\iiint_{-\infty}^{\infty} w^2 f_s d\underline{u}$$

with all off-diagonal elements equal to zero. Introducing the 1st-order CE expansion for f_s, we then get:

$$\lambda_{11}^s = \big(1-\nu_{ES}\big)\Big(\frac{k\hat{T}}{m_s}\Big) + \frac{\nu_{ES}}{n_s}\iiint_{-\infty}^{\infty}\big(u-u_s^{(g)}\big)^2 G_s^{ES} d\underline{u}$$
$$-\frac{\nu_{ES}}{n_s}\frac{\epsilon\big(1-\nu_{ES}\big)}{\nu}\iiint_{-\infty}^{\infty}\Big\{\big(u-u_0\big)^2 + 2\big(u-u_0\big)\big(u_0-u_s^{(g)}\big) + \big(u_0-u_s^{(g)}\big)^2\Big\}\Big(\frac{\partial f_s^M}{\partial t} + u\frac{\partial f_s^M}{\partial x} + v\frac{\partial f_s^M}{\partial y}\Big)d\underline{u}$$
$$\Rightarrow \lambda_{11}^s = \Big(\frac{k\hat{T}}{m_s}\Big) - \nu_{ES}\frac{\epsilon}{\nu}\frac{kT}{m_s}\frac{4}{3}\frac{\partial u_0}{\partial x} + O(\epsilon^2) \tag{70}$$

and for λ_{22}^s and λ_{33}^s:

$$\lambda_{22}^s = \big(1-\nu_{ES}\big)\Big(\frac{k\hat{T}}{m_s}\Big) + \frac{\nu_{ES}}{n_s}\iiint_{-\infty}^{\infty} v^2 G_s^{ES} d\underline{u} - \frac{\nu_{ES}}{n_s}\frac{\epsilon\big(1-\nu_{ES}\big)}{\nu}\iiint_{-\infty}^{\infty} v^2\Big(\frac{\partial f_s^M}{\partial t} + u\frac{\partial f_s^M}{\partial x} + v\frac{\partial f_s^M}{\partial y}\Big)d\underline{u}$$
$$\Rightarrow \lambda_{22}^s = \Big(\frac{k\hat{T}}{m_s}\Big) + \nu_{ES}\frac{\epsilon}{\nu}\frac{kT}{m_s}\frac{2}{3}\frac{\partial u_0}{\partial x} \quad ; \quad \lambda_{33}^s = \Big(\frac{k\hat{T}}{m_s}\Big) + \nu_{ES}\frac{\epsilon}{\nu}\frac{kT}{m_s}\frac{2}{3}\frac{\partial u_0}{\partial x} \tag{71}$$

Appendix C: CE Limit

The detailed derivation of the continuum limit of all three models is shown. Note that the mass and momentum limits of the original and Shakhov-based models are the same and is shown only for the corrected Shakhov model G_s^{Sh}.

Mass Equation

The time-derivative term has the following form for all the models:

$$\iiint_{-\infty}^{\infty} \Big\{ G_s^{Sh} - \frac{\epsilon}{\nu}\Big(\frac{\partial f_s^M}{\partial t} + u\frac{\partial f_s^M}{\partial x}\Big)\Big\} d\underline{u} = n_s \tag{72}$$
$$\iiint_{-\infty}^{\infty} \Big\{ G_s^{ES} - \frac{\epsilon(1-\nu_{ES})}{\nu}\Big(\frac{\partial f_s^M}{\partial t} + u\frac{\partial f_s^M}{\partial x}\Big)\Big\} d\underline{u} = n_s$$

The flux in the x-direction:

$$\iiint_{-\infty}^{\infty} u\Big\{ G_s^{Sh} - \frac{\epsilon}{\nu}\Big(\frac{\partial f_s^M}{\partial t} + u\frac{\partial f_s^M}{\partial x}\Big)\Big\} d\underline{u} = n_s u_s^{(g)} - \epsilon\frac{kT}{\nu}\Big[\frac{1}{m_s}\frac{\partial n_s}{\partial x} - \frac{n_s}{\rho}\frac{\partial n}{\partial x} + \frac{n_s}{T}\Big(\frac{1}{m_s} - \frac{n}{\rho}\Big)\frac{\partial T}{\partial x}\Big] \tag{73}$$
$$\iiint_{-\infty}^{\infty} u\Big\{ G_s^{ES} - \frac{\epsilon(1-\nu_{ES})}{\nu}\Big(\frac{\partial f_s^M}{\partial t} + u\frac{\partial f_s^M}{\partial x}\Big)\Big\} d\underline{u} = n_s u_s^{(g)} - \epsilon\frac{(1-\nu_{ES})kT}{\nu}\Big[\frac{1}{m_s}\frac{\partial n_s}{\partial x} - \frac{n_s}{\rho}\frac{\partial n}{\partial x} + \frac{n_s}{T}\Big(\frac{1}{m_s} - \frac{n}{\rho}\Big)\frac{\partial T}{\partial x}\Big]$$

The mass equation in the continuum limit after substituting the expression for $u_s^{(g)}$ is the same for all three models, as expected.

$$\frac{\partial n_s}{\partial t} + \frac{\partial}{\partial x}\Big\{ n_s u_0 - \epsilon\frac{kT}{\eta}\Big[\frac{1}{m_s}\frac{\partial n_s}{\partial x} - \frac{n_s}{\rho}\frac{\partial n}{\partial x} + \frac{n_s}{T}\Big(\frac{1}{m_s} - \frac{n}{\rho}\Big)\frac{\partial T}{\partial x}\Big]\Big\} = 0 \tag{74}$$

Momentum Equation

The time-derivative term has the following form for all the models:

$$\sum_{s=1}^{2}\iiint_{-\infty}^{\infty} m_s u\Big\{ G_s^{Sh} - \frac{\epsilon}{\nu}\Big(\frac{\partial f_s^M}{\partial t} + u\frac{\partial f_s^M}{\partial x}\Big)\Big\} d\underline{u} = \sum_{s=1}^{2} m_s n_s u_s^{(g)} = \sum_{s=1}^{2}\rho_s\Big[\Big(1-\frac{\eta}{\nu}\Big)u_s + \frac{\eta}{\nu}u_0\Big] = \rho u_0$$
$$\sum_{s=1}^{2}\iiint_{-\infty}^{\infty} m_s u\Big\{ G_s^{ES} - \frac{\epsilon(1-\nu_{ES})}{\nu}\Big(\frac{\partial f_s^M}{\partial t} + u\frac{\partial f_s^M}{\partial x}\Big)\Big\} d\underline{u} = \sum_{s=1}^{2} m_s n_s u_s^{(g)} \tag{75}$$
$$= \sum_{s=1}^{2}\rho_s\Big[\Big(1-\frac{\eta}{\nu}(1-\nu_{ES})\Big)u_s + \frac{\eta}{\nu}(1-\nu_{ES})u_0\Big] = \rho u_0$$

Here due to the summation, the contribution from the CE expansion is 0.

The inviscid flux in the x-direction:

$$\sum_{s=1}^{2}\iiint_{-\infty}^{\infty} m_s u^2 G_s^{Sh} d\underline{u} = \sum_{s=1}^{2} m_s n_s\Big(\frac{k\hat{T}}{m_s} + (u_s^{(g)})^2\Big) = nk\hat{T} + \sum_{s=1}^{2}\rho_s (u_s^{(g)})^2 = nkT + \rho u_0^2 + O(\epsilon^2) \tag{76}$$

$$\begin{aligned}\sum_{s=1}^{2}\iiint_{-\infty}^{\infty} m_s u^2 G_s^{ES} d\underline{u} = \sum_{s=1}^{2} m_s n_s(\lambda_{11}^s + (u_s^{(g)})^2) &= \sum_{s=1}^{2} m_s n_s\Big(\frac{k\hat{T}}{m_s} - \nu_{ES}\frac{\epsilon}{\nu}\frac{kT}{m_s}\frac{4}{3}\frac{\partial u_0}{\partial x} + (u_s^{(g)})^2 + O(\epsilon^2)\Big)\\ &= nkT + \rho u_0^2 - \nu_{ES}\frac{\epsilon}{\nu} nkT\frac{4}{3}\frac{\partial u_0}{\partial x} + O(\epsilon^2)\end{aligned}$$

The viscous part for all models is similar, with the ES model pre-multiplied as always by $(1-\nu_{ES})$

$$\sum_{s=1}^{2}\iiint_{-\infty}^{\infty} m_s u^2\Big\{\frac{\epsilon}{\nu}\Big(\frac{\partial f_s^M}{\partial t} + u\frac{\partial f_s^M}{\partial x}\Big)\Big\} d\underline{u} = \frac{\epsilon}{\nu} nkT\frac{4}{3}\frac{\partial u_0}{\partial x} \tag{77}$$

The momentum equation results in:

$$\frac{\partial \rho u_0}{\partial t} + \frac{\partial}{\partial x}\Big\{nkT + \rho u_0^2 - \mu\frac{4}{3}\frac{\partial u_0}{\partial x}\Big\} = 0 \tag{78}$$

where the viscosity coefficient $\mu = \frac{\epsilon}{\nu} nkT$

Energy Equation

The time-derivative term has the form:

$$\sum_{s=1}^{2}\iiint_{-\infty}^{\infty} m_s \frac{1}{2}(u^2+v^2+w^2)\Big\{G_s - \frac{\epsilon}{\nu}\Big(\frac{\partial f_s^M}{\partial t} + u\frac{\partial f_s^M}{\partial x}\Big)\Big\} d\underline{u} = \sum_{s=1}^{2}\Big\{n_s m_s\Big(\frac{1}{2}(u_s^{(g)})^2 + \frac{3}{2}\frac{k\hat{T}}{m_s}\Big)\Big\} \tag{79}$$

$$\sum_{s=1}^{2}\iiint_{-\infty}^{\infty} m_s \frac{1}{2}(u^2+v^2+w^2)\Big\{G_s^{Sh} - \frac{\epsilon}{\nu}\Big(\frac{\partial f_s^M}{\partial t} + u\frac{\partial f_s^M}{\partial x}\Big)\Big\} d\underline{u} = \sum_{s=1}^{2}\Big\{n_s m_s\Big(\frac{1}{2}(u_s^{(g)})^2 + \frac{3}{2}\frac{k\hat{T}}{m_s}\Big)\Big\}$$

$$\begin{aligned}\sum_{s=1}^{2}\iiint_{-\infty}^{\infty} m_s \frac{1}{2}(u^2+v^2+w^2)\Big\{G_s^{ES} - \frac{\epsilon}{\nu}(1-\nu_{ES})\Big(\frac{\partial f_s^M}{\partial t} + u\frac{\partial f_s^M}{\partial x}\Big)\Big\} d\underline{u} &= \sum_{s=1}^{2}\Big\{n_s m_s\Big(\frac{1}{2}(u_s^{(g)})^2 + \lambda_{11}^s + \lambda_{22}^s + \lambda_{33}^s\Big)\Big\}\\ &= \sum_{s=1}^{2}\Big\{n_s m_s\Big(\frac{1}{2}(u_s^{(g)})^2 + \frac{3}{2}\frac{k\hat{T}}{m_s} + O(\epsilon^2)\Big)\Big\}\end{aligned}$$

For the 0th-order part of the flux in the $x-$direction this results in,

$$\begin{aligned}
\sum_{s=1}^{2}\iiint_{-\infty}^{\infty} m_s u\frac{1}{2}(u^2+v^2+w^2)G_s d\underline{u} &= \sum_{s=1}^{2}\Big\{n_s m_s\Big(\frac{1}{2}(u_s^{(g)})^3+\frac{5}{2}\frac{k\hat{T}}{m_s}u_s^{(g)}\Big)\Big\} \\
\sum_{s=1}^{2}\iiint_{-\infty}^{\infty} m_s u\frac{1}{2}(u^2+v^2+w^2)G_s^{Sh} d\underline{u} &= \sum_{s=1}^{2}\Big\{n_s m_s\Big(\frac{1}{2}(u_s^{(g)})^3+\frac{5}{2}\frac{k\hat{T}}{m_s}u_s^{(g)}+\frac{(1-Pr)q_{x_s}^{corr}}{m_s}\Big)\Big\} \\
\sum_{s=1}^{2}\iiint_{-\infty}^{\infty} m_s u\frac{1}{2}(u^2+v^2+w^2)G_s^{ES} d\underline{u} &= \sum_{s=1}^{2}\Big\{n_s m_s\frac{1}{2}\Big((u_s^{(g)})^2+3\lambda_{11}^s+\lambda_{22}^s+\lambda_{33}^s\Big)\Big\} \\
&= \sum_{s=1}^{2}\Big\{n_s m_s\Big(\frac{1}{2}(u_s^{(g)})^3+\frac{5}{2}\frac{k\hat{T}}{m_s}u_s^{(g)}-\nu_{ES}\frac{\epsilon}{\nu}\frac{4}{3}\frac{kT}{m_s}u_s^{(g)}\frac{\partial u_0}{\partial x}+O(\epsilon^2)\Big)\Big\}
\end{aligned} \tag{80}$$

The 1-st order part of the flux in the x-direction is based on the Maxwellian and is common for all the models, except a multiplication by $(1-\nu_{ES})$ for the ES model. The common part results in:

$$\begin{aligned}
&\sum_{s=1}^{2}\iiint_{-\infty}^{\infty} m_s u\frac{1}{2}(u^2+v^2+w^2)\Big\{\frac{\epsilon}{\nu}\Big(\frac{\partial f_s^M}{\partial t}+u\frac{\partial f_s^M}{\partial x}\Big)\Big\}d\underline{u} \\
&= \sum_{s=1}^{2} m_s\frac{\epsilon}{\nu}\left[\frac{\eta}{\epsilon}n_s\Big(\frac{3}{2}u_0^2+\frac{5}{2}\frac{kT}{m_s}\Big)(u_0-u_s)+\frac{4}{3}n_s\frac{kT}{m_s}u_0\frac{\partial u_0}{\partial x}+\frac{5}{2}n_s\Big(\frac{kT}{m_s}\Big)^2\frac{1}{T}\frac{\partial T}{\partial x}\right]
\end{aligned} \tag{81}$$

Combining the time-derivative and the flux terms forms the limit of the energy equation up to order $O(\epsilon^2)$ for each model as shown in the text.

References

1. Andries P., Aoki K., Perthame B. A consistent BGK-type model for gas mixtures. *Journal of Statistical Physics*. 2002;106(5):993–1018.

2. Andries P., Perthame B. The ES-BGK model equation with correct Prandtl number. *AIP Conference Proceedings*. 2001;585(1):30–36.

3. Andries P., Tallec P. Le, Perlat J., Perthame B. The Gaussian-BGK model of Boltzmann equation with small Prandtl number. *European Journal of Mechanics - B/Fluids*. 2000;19(6):813 –830.

4. Belcher J. R., Slaton W. V., Raspet R., Bass H. E., Lightfoot J. Working gases in thermoacoustic engines. *The Journal of the Acoustical Society of America*. 1999;105(5):2677–2684.

5. Bhatnagar P. L., Gross E. P., Krook M. A model for collision processes in gases. I. Small amplitude processes in charged and neutral one-component systems. *Phys. Rev.* 1954;94:511–525.

6. Bird G.A. *Molecular gas dynamics and the direct simulation of gas flows*: Oxford Science Publications; 1994.

7. Bobylev A. V., Bisi M., Groppi M., Spiga G., Potapenko I. F. A general consistent BGK model for gas mixtures. *Kinetic & Related Models*. 2018;11(6):1377 –1393.

8. Brull S. An Ellipsoidal Statistical Model for gas mixtures. *Communications in Mathematical Sciences*. 2015;13(1):1 –13.

9. Brull S., Pavan V., Schneider J. Derivation of a BGK model for mixtures. *European Journal of Mechanics - B/Fluids*. 2012;33:74 –86.

10. Brull S., Schneider J. A new approach for the Ellipsoidal Statistical Model. *Continuum Mechanics and Thermodynamics*. 2008;20(2):63 –74.

11. Brull S., Schneider J. On the Ellipsoidal Statistical Model for polyatomic gases. *Continuum Mechanics and Thermodynamics*. 2009;20(8):489 –508.

12. Center R. E. Measurement of shock wave structure in helium argon mixtures. *The Physics of Fluids*. 1967;10(8):1777–1784.

13. Chapman S., Cowling T.G. *The mathematical theory of non-uniform gases*. 2nd ed.: Cambridge University Press,London; 1952.

14. Chen S., Xu K., Cai Q. A comparison and unification of Ellipsoidal Statistical and Shakhov BGK models. *Advances in Applied Mathematics and Mechanics*. 2015;7(2):245–266.

15. Chigullapalli S., Venkattraman A., Ivanov M.S., Alexeenko A.A. Entropy considerations in numerical simulations of non-equilibrium rarefied flows. *Journal of Computational Physics*. 2010;229(6):2139 –2158.

16. Garzo V., Santos A., Brey J. J. A kinetic model for a multicomponent gas. *Physics of Fluids A: Fluid Dynamics*. 1989;1(2):380–383.

17. Goldman E., Sirovich L. Equations for gas mixtures. *The Physics of Fluids*. 1967;10(9):1928–1940.

18. Goldman E., Sirovich L. The structure of shock-waves in gas mixtures. *Journal of Fluid Mechanics*. 1969;35(3):575–597.

19. Groppi M., Monica S., Spiga G. A kinetic ellipsoidal BGK model for a binary gas mixture. *EPL (Europhysics Letters)*. 2011;96(6):64002.

20. Gross E. P., Krook M. Model for collision processes in gases: Small-amplitude oscillations of charged two-component systems. *Phys. Rev.* 1956;102(3):593 –604.

21. Haack J. R., Hauck C. D., Murillo M. S. A conservative, entropic multispecies BGK model. *Journal of Statistical Physics*. 2017;168(4):826–856.

22. Hamel B.B. Kinetic model for binary gas mixtures. *The Physics of Fluids*. 1965;8(3):418–425.

23. Harnett L. N., Muntz E. P. Experimental investigation of normal shock wave velocity distribution functions in mixtures of argon and helium. *The Physics of Fluids*. 1972;15(4):565–572.

24. Harten Ami. High resolution schemes for hyperbolic conservation laws. *Journal of Computational Physics*. 1983;49(3):357 –393.

25. Hirschfelder J. O., Curtiss C. F., Bird R. B. *Molecular theory of gases and liquids*. 1st ed.: Wiley, New York; 1954.

26. Holway, Jr. L. H. Kinetic theory of shock structure using an ellipsoidal distribution function. 1965:193–215.

27. Homolle Thomas M.M., Hadjiconstantinou Nicolas G. A low-variance deviational simulation Monte Carlo for the Boltzmann equation. *Journal of Computational Physics*. 2007;226(2):2341 –2358.

28. Klingenberg C., Pirner M. Existence, uniqueness and positivity of solutions for BGK models for mixtures. *Journal of Differential Equations*. 2018;264:702–727.

29. Klingenberg C., Pirner M., Puppo G. A consistent kinetic model for a two-component mixture with an application to plasma. *Kinetic & Related Models*. 2017;10(2):445–465.

30. Kosuge S., Aoki K., Takata S. Shock-wave structure for a binary gas mixture: finite-difference analysis of the Boltzmann equation for hard-sphere molecules. *European Journal of Mechanics - B/Fluids*. 2001;20(1):87 –126.

31. Morse T. F. Kinetic model equations for a gas mixture. *The Physics of Fluids*. 1964;7(12):2012–2013.

32. Sanders R.H., Prendergast K.H. The possible relation of the 3-kiloparsec arm to explosions in the galactic nucleus. *The Astrophysical Journal*. 1974;188.

33. Shakhov E. M. Generalization of the Krook kinetic relaxation equation. *Fluid Dynamics*. 1968;3(5):95–96.

34. Sharipov F., Strapasson J. L. Benchmark problems for mixtures of rarefied gases. I. Couette flow. *Physics of Fluids*. 2013;25(2):027101.

35. Sherman F. S. Shock-wave structure in binary mixtures of chemically inert perfect gases. *Journal of Fluid Mechanics*. 1960;8(3):465–480.

36. Sirovich L. Kinetic modeling of gas mixtures. *The Physics of Fluids*. 1962;5(8):908–918.

37. Wang R., Xu K. Unified gas-kinetic scheme for multi-species non-equilibrium flow. *AIP Conference Proceedings*. 2014;1628(1):970–975.

38. Weissman S., Mason E. A. Determination of gaseous-diffusion coefficients from viscosity measurements. *The Journal of Chemical Physics*. 1962;37(6):1289–1300.

39. Wilson C. D., Agarwal R. K., Tcheremissine F. G. Computation of hypersonic shock waves in inert gas mixtures using the Generalized Boltzmann equation. *AIP Conference Proceedings*. 2011;1333(1):152–157.

40. Wu L., Zhang J., Reese J. M., Zhang Y. A fast spectral method for the Boltzmann equation for monatomic gas mixtures. *Journal of Computational Physics*. 2015;298:602 –621.

41. Xu K. A gas-kinetic BGK scheme for the Navier-Stokes equations and its connection with artificial dissipation and Godunov method. *Journal of Computational Physics*. 2001;171(1):289 –335.

42. Xu K., Mao M., Tang L. A multidimensional gas-kinetic BGK scheme for hypersonic viscous flow. *Journal of Computational Physics*. 2005;203(2):405 –421.

43. Zhang Y., Zhu L., Wang R., Guo Z. Discrete unified gas kinetic scheme for all Knudsen number flows. III. Binary gas mixtures of Maxwell molecules. *Phys. Rev. E*. 2018;97:053306.